INFLUENCE OF SHEAR REINFORCEMENT ON REINFORCED CONCRETE CONTINUOUS DEEP BEAMS

K. H. Yang[a], H. S. Chung[b] and A. F. Ashour[c]

[a] *Corresponding author, Department of Architectural Engineering, Mokpo National University, Mokpo, Jeonnam, South Korea*

[b] *Department of Architectural Engineering, Chungang University, Seoul, South Korea*

[c] *School of Engineering, Design and Technology, University of Bradford, U.K.*

Biography: K. H. Yang is currently a visiting research fellow at the University of Bradford, UK and an assistant professor at Mokpo National University, Korea. He received his MSc and PhD degrees from Chungang University, Korea. His research interests include ductility, strengthening and shear of reinforced high-strength concrete structures.

H. S. Chung is a professor at Chungang University, Korea. He received his MSc and PhD degrees from Tokyo Institute of Technology, Japan. His research interests include flexure, shear and bond behavior of reinforced high-strength concrete members

A.F.Ashour is currently a senior lecturer at the University of Bradford, UK. He obtained his BSc and MSc degrees from Mansoura University, Egypt and his PhD from Cambridge University, UK. His research interests include shear, plasticity and optimisation of reinforced concrete and masonry structures.

ABSTRACT

Test results of twenty four reinforced concrete continuous deep beams are reported. The main variables studied were concrete strength, shear span-to-overall depth ratio and the amount and configuration of shear reinforcement. The results of this study show that the load transfer capacity of shear reinforcement was much more prominent in continuous deep beams than in simply supported deep beams. For beams having shear span-to-overall depth ratio of 0.5, horizontal shear reinforcement was always more effective than vertical shear reinforcement. The ratio of the load capacity measured and that predicted by the strut-and-tie model recommended by ACI 318-05 dropped against the increase of shear span-to-overall depth ratio. This decrease rate was more remarkable in continuous deep beams than that in simple deep beams. The strut-and-tie model recommended by ACI 318-05 overestimated the strength of continuous deep beams having shear span-to-overall depth ratio more than 1.0.

Keywords: continuous deep beams, shear reinforcement, load capacity, shear span-to-overall depth ratio, strut-and-tie model, ACI 318-05.

INTRODUCTION

Reinforced concrete deep beams are used in structures as load distribution elements such as transfer girders, pile caps and foundation walls in tall buildings. Although these members commonly have several supports, extensive experimental investigations have brought simple deep beams into focus. The behaviour of continuous deep beams is significantly different from that of simply supported deep beams. The coexistence of high shear and high moment within the interior shear span in continuous deep beams has a considerable effect on the development of cracks, leading to a significant reduction in the effective strength of the concrete strut which is the main load transfer element in deep beams[1]. Indeed, few experiments[1-3] were carried out on continuous deep beams of

2

shear span-to-overall depth ratio greater than 1.08. However the results of simple deep beams tested by Tan et al.[4], and Smith and Vantsiotis[5] showed that the effectiveness of horizontal and vertical shear reinforcement on controlling diagonal cracks and load transfer critically shifted for shear span-to-overall depth ratios not exceeding 1.0. Therefore a reasonable evaluation of the influence of shear reinforcement on continuous deep beams having shear span-to-overall depth ratios less than 1.0 requires further investigation.

The current codes, ACI 318-05[6], CSA-1994[7], and FIP-Recommendations 1999[8], and several researchers[9-11] have recommended the design of deep beams using the strut-and-tie model. In these strut-and-tie models, the main objective of shear reinforcement is to restrain the diagonal cracks near the ends of bottle-shaped struts and to give some ductility to struts. ACI 318-05 (Sec. A. 3. 3) allows the use of an effectiveness factor of 0.75 when computing the effective concrete compressive strength of bottle-shaped struts with reinforcement satisfying ACI 318-05 (Sec. A. 3.3). The value of the effectiveness factor drops to 0.6 if shear reinforcement as recommended by ACI 318-05 (Sec. A. 3.3) is not provided. This indicates that shear reinforcement satisfying ACI 318-05 (Sec. A. 3.3) allows the ultimate strength of beams predicted by the strut-and-tie model to be increased by 25%. However, studies on the validity of the strut-and-tie model recommended by the ACI 318-05 are very rare even in simple deep beams[12, 13].

This paper presents test results of twenty four two-span reinforced concrete deep beams. The main variables included concrete strength, shear span-to-overall depth ratio, and the amount and configuration of shear reinforcement. The influence of shear reinforcement on the ultimate shear strength in continuous deep beams was compared to that in the corresponding simple ones. The load capacity predictions of reinforced concrete continuous deep beams by the strut-and-tie model of ACI 318-05 were evaluated by comparison with test results.

RESEARCH SIGNIFICANCE

A great deal of research has focused on simply supported deep beams. Even the few tests on continuous deep beams were carried out on beams having shear span-to-overall depth ratio exceeding 1.0 and concrete strength of less than 35 MPa (5.0 ksi). Test results in this study clearly showed the influence of shear reinforcement on the structural behavior of continuous deep beams according to the variation of concrete strength and shear span-to-overall depth ratio. The ultimate shear strength of continuous deep beams and load transfer capacity of shear reinforcement were compared to those of the corresponding simple deep beams and the predictions obtained from the strut-and-tie model recommended in ACI 318-05.

EXPERIMENTAL INVESTIGATION

The details of geometrical dimensions and reinforcement of test specimens are shown in Table 1 and Fig. 1. The main variables studied were compressive strength of concrete, $f_c^{'}$, shear span-to-overall depth ratio, a/h, and the amount and configuration of shear reinforcement. Beams tested were classified into two groups according to the concrete compressive strength: L-series for design concrete strength of 30 MPa (4350 psi) and H-series for design concrete strength of 60 MPa (8700 psi). The shear span-to-overall depth ratios were initially designed to be 0.5 and 1.0 to allow comparison of current results with those reported by Yang[13] for simple deep beams. However a/h in H-series was increased from 0.5 to 0.6, as the capacity of beams having $f_c^{'}$ of 60 MPa (8700 psi) and a/h of 0.5 had exceeded the capacity of the loading machine in the pilot test. The configuration of shear reinforcement included four different arrangements as shown in Fig. 1: none, only vertical, only horizontal, and orthogonal reinforcement. The spacing of shear reinforcement was chosen to be 60 mm (2.36 in.) and 120 mm (4.72 in.) and the corresponding shear

reinforcement ratios, ρ $\left(= \dfrac{A_s}{b_w s}\right.$, where A_s = area of shear reinforcement at spacing s and b_w =

beam width), were 0.003 and 0.006, respectively, in order to satisfy the maximum spacing specified

in ACI 318-05 (Sec. 11.8) and the minimum amount recommended in ACI 318-05 (Sec. A 3.3.2).

The beam notation given in Table 1 includes four parts. The first part refers to the concrete design

strength: L for low compressive strength and H for high compressive strength. The second part is

used to identify the shear span-to-overall depth ratio. The third and fourth parts give the amount of

horizontal and vertical shear reinforcement, respectively: N for no shear reinforcement, S and T for

shear reinforcement ratios of 0.003 and 0.006, respectively. For example, L5-SS is a continuous

deep beam having design concrete strength of 30 MPa (4350 psi), shear span-to-overall depth ratio

of 0.5, and both horizontal and vertical shear reinforcement ratios of 0.003.

All tested beams had the same section width and overall depth: the section width, b_w, of 160 mm

(6.3 in.) and overall depth, h, of 600 mm (23.6 in.). Both longitudinal top, $\rho_s' \left(= \dfrac{A_{st}'}{b_w d}\right)$, and bottom,

$\rho_s \left(= \dfrac{A_{st}}{b_w d}\right)$, reinforcement ratios were kept constant in all beams as 1%, which were calculated

from the non-linear FE analysis software[4], to ensure no flexural yield of longitudinal reinforcement

prior to failure of the concrete strut. The length of each span, L, varied according to a/h ratio as

given in Table 1. The clear cover to longitudinal top and bottom reinforcement was 35 mm (1.38

in.). The longitudinal bottom reinforcement was continuous over the full length of the beam and

welded to 160×100×10 mm (6.3×3.9×0.39 in.) end plates. The longitudinal top reinforcement was

anchored in the outside of the exterior support by 90° hook according to ACI 318-05. The vertical

shear reinforcement was closed stirrups and the horizontal shear reinforcement with 90° hook was

arranged along the longitudinal axis in both sides of the beams.

Material properties

The mechanical properties of reinforcement are given in Table 2. All longitudinal and shear reinforcing bars were deformed bars with a 19 mm (0.75 in.) diameter having yield strength of 562 MPa (81.6 ksi) and a 6 mm (0.23 in.) diameter having yield strength of 483 MPa (70 ksi), respectively. The yield stress of 6 mm (0.23 in.) diameter reinforcement was obtained by 0.2 % offset method.

The ingredients of ready-mixed concrete were ordinary portland cement, fly-ash, irregular gravel of a maximum size of 25 mm, and sand. The water-binder ratios of L-series added with fly-ash of 12% and of H-series added with fly-ash of 20% were 0.41 and 0.27, respectively. All specimens were cast in a vertical position in the same wooden mould. Control specimens which were 100 mm (3.94 in.) diameter × 200 mm (7.87 in.) high cylinder were cast and cured simultaneously with beams in order to determine the compressive strength. They were tested soon after the beam test. The results of the cylinder compressive strength given in Table 1 are the average value from testing nine cylinders.

Test set-up

Loading and instrumentation arrangements are shown in Fig. 2. All beams having two spans were tested to failure under a symmetrical two-point top loading system with loading rate of 30 kN/min (6.7 klb/min) using a 3000 kN (675 klb) capacity universal testing machine (UTM). Each span was identified as E-Span or W-span as shown in Fig. 1. The two exterior end supports are designed to allow horizontal and rotational movements, whereas the intermediate support prevents horizontal movement but allows rotation. In order to evaluate the shear force and loading distribution, 1000 kN (225 klb) capacity load cells were installed in both exterior end supports. At the location of loading or support point, a steel plate of 100 mm (3.94 in.), 150 mm (5.9 in.) or 200 mm (7.88 in.) wide was provided to prevent premature crushing or bearing failure, as shown in Fig. 2. All beams were

6

preloaded up to a total load of 150 kN (33.7 klb) before testing, which wouldn't produce any cracks, in order to assure a similar loading distribution to supports according to the result of linear two-dimensional finite element (2-D FE) analysis.

Vertical deflections at a distance of $0.45L \sim 0.47L$ from the exterior support, which is the location of the maximum deflection predicted by the linear 2-D FE analysis, and at the mid-span of each span were measured using linear variable differential transformers (LVDTs). Both surfaces of the beams tested were whitewashed to aid on the observation of crack development during testing. The inclined crack width of concrete struts joining the edges of load and support plates was monitored by the PI type gages as shown in Fig. 2. The strains of shear reinforcement were measured by 5 mm (0.2 in.) electrical resistance strain gages (ERS) at the region crossing the line joining the edges of load and intermediate support plates as shown in Fig. 1. At each load increment, the test data were captured by a data logger and automatically stored.

Support settlements

Continuous deep beams are sensitive to differential support settlements causing additional moment and shear. To assess the effect of differential settlements on the beams tested, a linear 2-D FE analysis considering shear deformation effect was performed on the beams shown in Fig. 1. For the beams tested, sources of relative support settlements were the elastic shortening of the load cell and plates, and elastic deformation of the bed of UTM. The second moment of area of the UTM bed cross section about the bending axis is 3.2×10^{10} mm^4 (7.69×10^4 in.^{4}), then the elastic deformation under a point load R (in kN) at a distance 1500 mm (59 in.) from the center of UTM is $0.000176R$ mm. The amount of elastic shortening due to a load at the exterior and intermediate supports involving the load cell and plates was considered in designing the support size. When a/h ratio is 0.5, the reactions of the exterior and intermediate supports due to the total applied load P, from the linear 2-D FE analysis, are $0.2P$ and $0.6P$, respectively. As the height of the intermediate support

is equal to that of the exterior load cell, the contact area of the intermediate support with the UTM bed was designed to be three times wider than that of the load cell at the exterior support to produce the same elastic shortening. The pilot test results showed that the maximum settlement of the exterior support relative to the intermediate support was in order of $L/25000$. For a differential settlement between the exterior and intermediate supports of $L/25000$, the maximum additional shear forces obtained from linear 2-D FE analysis are 25 kN (5.62 klb) and 7 kN (1.57 klb) for beams having a/h ratio of 0.5 and 1.0, respectively. This indicates that the differential settlement had no significant effect on the test arrangement.

EXPERIMENTAL RESULTS AND DISCUSSION

Crack propagation and failure mode

The crack propagation was significantly influenced by the shear span-to-overall depth ratio as shown in Fig. 3 and Table 3. The crack pattern in L-series was similar to that in H-series, therefore it is not shown in Fig. 3. For beams with a/h = 0.5, the first crack suddenly developed in the diagonal direction at about 40% of the ultimate strength at the mid-depth of the concrete strut within the interior shear span, and then a flexural crack in the sagging region immediately followed. The first flexural crack over the intermediate support generally occurred at about 80% of the ultimate strength, and its development height at failure was below $0.2h$. As the load increased, more flexural and diagonal cracks were formed and a major diagonal crack extended to join the edges of the load and intermediate support plates. A diagonal crack within the exterior shear span occurred suddenly near the failure load. Cracks in beams with a/h=1.0 developed in a different order from that described above for beams with a/h=0.5 as the first crack occurred vertically in the hogging zone, followed by a diagonal crack in the interior shear span, then a vertical crack took place in the sagging zone. Also diagonal cracks within the exterior shear span are seldom developed in beams

8

with a/h =1.0. The influence of shear reinforcement on the first flexural and diagonal crack loads was not significant (see Table 3) as also observed in simple deep beams given in appendix A.

Just before failure, the two spans showed nearly the same crack patterns. All beams developed the same mode of failure as observed in other experiments[3]. The failure planes evolved along the diagonal crack formed at the concrete strut along the edges of the load and intermediate support plates. Two rigid blocks separated from original beams at failure due to the significant diagonal crack. An end block rotated about the exterior support leaving the other block fixed over the other two supports as shown in Fig. 3.

Load versus mid-span deflection

The beam deflection at mid-span was less than that measured at $0.45L \sim 0.47L$ from the exterior support until the occurrence of the first diagonal crack as predicted by the 2-D FE analysis. However, after the first diagonal crack, the mid-span deflection was higher. Therefore, the mid-span deflection of failed span for different beams tested are only presented in Fig. 4 against the total applied load: Fig. 4 (a) for beams in L-series and Fig. 4 (b) for beams in H-series. The initial stiffness of beams tested increased in accordance with the increase of concrete strength and the decrease of the shear span-to-overall depth ratio, but it seems to be independent of the amount and configuration of shear reinforcement. The development of flexural cracks in sagging and hogging zones has little influence on the stiffness of beams tested. But the occurrence of diagonal cracks in the interior shear span caused sharp decrease to the beam stiffness and increase of the beam deflection. This stiffness reduction was prominent in case of lower concrete strength and higher shear span-to-overall depth ratio.

Support reaction

Fig. 5 shows the amount of the load transferred to the end and intermediate supports against the total applied load in L-series beams. On the same figure, the support reactions obtained from the linear 2-D FE analysis are also presented. The relationship between the total applied load and support reaction in H-series beams was similar to that in L-series beams; therefore, not presented here. Before the first diagonal crack, the relationship of the end and intermediate support reactions against the total applied load in all beams tested shows good agreement with the prediction of the linear 2-D FE analysis. However the amount of loads transferred to the end support was slightly higher than that predicted by the linear 2-D FE analysis after the occurrence of the first diagonal crack within the interior shear span. At failure, the difference between the measured support reaction and prediction of the linear 2-D FE analysis was in order of 7% and 12 %, for beams with a/h=0.5 and a/h=1.0, respectively. The distribution of applied load to supports was independent of the amount and configuration of shear reinforcement. This means that although after the occurrence of diagonal cracks, the beam stiffness has reduced as shown in Fig. 4, the internal redistribution of forces is limited.

Width of diagonal crack

Fig. 6 shows the variation of the diagonal crack width in the interior shear span according to the configuration of shear reinforcement: Fig. 6 (a) at the first diagonal cracking load and Fig. 6 (b) at the same load as the ultimate failure load of the corresponding beam without shear reinforcement. For the same concrete compressive strength, the larger the shear span-to-overall depth ratio, the wider the diagonal crack width. Shear reinforcement had an important role in restraining the development of the diagonal crack width, which significantly depended on the shear span-to-overall depth ratio. The reduction of diagonal crack width was prominent in beams with horizontal shear reinforcement only or orthogonal shear reinforcement and with vertical shear reinforcement only

when shear span-to-overall depth ratios were 0.5 and 1.0, respectively. For beams with a/h=1.0, a smaller diagonal crack width was observed in beams with vertical shear reinforcement only than in beams with orthogonal shear reinforcement, even though the total shear reinforcement ratio in these beams was the same ($\rho_v + \rho_h = 0.006$). It seems to be possible to reduce the diagonal crack width by more than twice if shear reinforcement is suitably arranged according to the variation of shear span-to-overall depth ratio.

Fig. 7 shows the strain in shear reinforcement against the diagonal crack width in H-series beams: Fig. 7 (a) for vertical shear reinforcement in beams having either vertical or orthogonal shear reinforcement, and Fig. 7 (b) for horizontal shear reinforcement in beams having either horizontal or orthogonal shear reinforcement. The relation between stains in shear reinforcement and the diagonal crack width in L-series beams was similar to that in H-series beams; therefore, not presented here. The strains of shear reinforcement were recorded by ERS gages at different locations as shown in Fig. 1. Shear reinforcement was not generally strained at initial stages of loading. However, strains suddenly increased with the occurrence of the first diagonal crack. In beams with a/h=0.6, only horizontal reinforcing bars reached its yield strength, whereas in beams with a/h=1.0, only vertical reinforcing bars yielded. This indicates that the reinforcement ability to transfer tension across cracks, which is a function of the crack width, strongly depends on the angle between the reinforcement and the axis of the strut.

Ultimate shear stress

The normalized ultimate shear strength, $\lambda = \dfrac{V_n}{b_w d \sqrt{f_c{}'}}$, plotted against the shear span-to-overall depth ratio is given in Fig. 8: Fig. 8 (a) for simple deep beams given in appendix A, and Fig. 8 (b) for continuous deep beams including Ashour's and Rogowsky et al.'s test results. It can be seen that the ultimate shear strength of all beams without or with shear reinforcement dropped due to the

11

increase of a/h ratio. The reduction of the ultimate shear strength was also dependent on the configuration of shear reinforcement. For deep beams without shear reinforcement, the normalized ultimate shear strength, λ, in continuous deep beams was less than that in simple ones by an average of 26% due to higher transverse tensile strains produced by the tie action of longitudinal top and bottom reinforcement. When shear reinforcement is provided, the normalized ultimate shear strength, λ, in continuous deep beams matched that of the corresponding simple ones. The influence of the horizontal and vertical shear reinforcement on the ultimate shear strength is influenced by the shear span-to-overall depth ratio. The lower the shear span-to-overall depth ratio, the more effective the horizontal shear reinforcement and the less effective the vertical shear reinforcement. When a/h ratio was below 0.6, the shear strength of deep beams with minimum horizontal shear reinforcement had an average of 150 % higher than the upper bound value, $0.83\sqrt{f_c'}b_w d$, specified in ACI 318-05 (Sec. 11.8.3).

Load transfer capacity of shear reinforcement

The shear strength of deep beams, V_n, can be frequently described as follows:

$$V_n = V_c + V_s \tag{1}$$

where V_c and V_s = load capacity of concrete and the load transfer capacity of shear reinforcement, respectively.

As the load capacity of concrete is usually regarded as the strength of beams without shear reinforcement, $(V_n)_{W/O}$, the ratio of the load transfer capacity of shear reinforcement to the shear strength of beams, V_s/V_n, is

$$\frac{V_s}{V_n} = \frac{V_n - (V_n)_{W/O}}{V_n} \tag{2}$$

The variations of V_s/V_n at failed shear span against the increase of a/h ratio are given in Fig. 9: Fig. 9 (a), (b), and (c) for beams with vertical shear reinforcement only, with horizontal shear reinforcement only, and with orthogonal shear reinforcement, respectively. On the same figure, the test results of simple deep beams given in appendix A, which had the same material and geometrical properties as continuous deep beams tested in the current study, are also presented. The load transfer capacity of shear reinforcement is more pronounced in continuous deep beams than that in simple ones.

The load transfer capacity of shear reinforcement is dependent on the shear span-to-overall depth ratio, a/h. The load transfer capacity of vertical shear reinforcement was higher in beams having a/h=1.0 than those having a/h=0.5 as shown in Fig. 9 (a). On the other hand, the load transfer capacity of horizontal shear reinforcement was higher in beams having a/h=0.5 than those having a/h=1.0 as shown in Fig. 9 (b). Existing test results of continuous deep beams carried out by Rogowsky et al[1] and Ashour[2], and the comments of ACI 318-05 (Sec 11.8) have suggested that horizontal shear reinforcement have little influence on the shear strength improvement and crack control. In the current tests, horizontal shear reinforcement is more effective than vertical shear reinforcement for beams with shear span-to-overall depth ratio of 0.5 as shown in Fig. 8 and Fig. 9.

Comparison with Current Codes

It has been shown by several researchers, Rogowsky et al[1], Ashour[2], and Tan et al.[4], that the shear capacity prediction of reinforced concrete deep beams obtained from ACI 318-99[15] (unchanged since ACI 318-83) was unconservative. For the design of deep beams, ACI 318-05 has recommended the use of either nonlinear analysis or strut-and-tie model. Fig. 10 shows a strut-and-tie model of continuous deep beams in accordance with ACI 318-05 Appendix A. The strut-and-tie model shown in Fig. 10 identifies two main load transfer systems: one of which is the strut-and-tie

action formed with the longitudinal bottom reinforcement acting as a tie and the other is the strut-and-tie action due to the longitudinal top reinforcement. As the applied loads in the two-span continuous deep beams are carried to supports through concrete struts of exterior and interior shear spans (see Fig. 10), the total load capacity of two-span continuous deep beams, P_n, due to failure of concrete struts is

$$P_n = 2(F_E + F_I)\sin\theta \qquad (3)$$

where F_E, and F_I = load capacities of exterior and interior concrete struts, respectively, and θ = the angle between the concrete strut and the longitudinal axis of the deep beam, which can be expressed as $\tan^{-1}(jd/a)$. The distance between the center of top and bottom nodes, jd, could be approximately assumed as the distance between the center of longitudinal top and bottom reinforcing bars as below:

$$jd = h - c - c' \qquad (4)$$

where h = overall section depth, c and c' = the cover of longitudinal bottom and top reinforcement, respectively, as shown in Fig. 10.

The nodes at the applied load point could be classified as a CCC type, which is a hydrostatic node connecting both exterior and interior compressive struts. It was proved by Marti[10] that the width of the strut at a CCC node is in proportion to the principal stress normal to the node face to make the state of stress in the whole node region constant. The loading plate width can be subdivided into two parts in accordance with the ratio of the exterior reaction to the applied load, β, each to form the node connecting the exterior and the interior struts, respectively. The values β of tested beams are 0.4 and 0.346 when a/h ratios are 0.5 and 1.0, respectively as estimated from the linear 2-D FE analysis. If enough anchorage of longitudinal reinforcement is provided, average widths of concrete struts in interior, $(w_s)_I$, and exterior shear spans, $(w_s)_E$, are

$$(w_s)_I = \frac{(w_t' + 2c')\cos\theta + \left[0.5(l_p)_I + (1.0 - \beta)(l_p)_P\right]\sin\theta}{2} \qquad \text{(5-a)}$$

$$(w_s)_E = \frac{(w_t' + 2c')\cos\theta + \left[(l_p)_E + \beta(l_p)_P\right]\sin\theta}{2} \qquad \text{(5-b)}$$

where $(l_p)_P$, $(l_p)_E$ and $(l_p)_I$ = widths of loading, exterior support and interior support plates, respectively, and w_t' = the smaller of the height of the plate anchored to longitudinal reinforcement, w_t, and twice of the cover of longitudinal bottom reinforcement, $2c$, as shown in Fig. 10.

The load transfer capacity of the concrete strut depends on the area of the strut and the effective concrete compressive strength. Hence, the load capacities of the exterior and interior concrete struts are

$$F_E = v_e f_c' b_w (w_s)_E \qquad \text{(6-a)}$$

$$F_I = v_e f_c' b_w (w_s)_I \qquad \text{(6-b)}$$

where v_e = the effectiveness factor of concrete. The shear capacity at the interior shear span, $(V_n)_I$, where the failure is expected to occur in continuous deep beams can be calculated from $F_I \sin\theta$.

The minimum amount of shear reinforcement required in bottle-shaped struts, which is recommended to be placed in two orthogonal directions in each face, is suggested by ACI 318-05 as follows

$$\sum \frac{A_{si}}{b_w s_i} \sin\alpha_i \geq 0.003 \qquad \text{(7)}$$

where A_{si}, and s_i = the total area and spacing in the i–th layer of reinforcement crossing a strut, respectively, and α_i = the angle between i–th layer of reinforcement and the strut.

The effectiveness factors for concrete strength not exceeding 40 MPa (5.8 ksi) in ACI 318-05 are suggested as 0.75 and 0.6 when shear reinforcement satisfying Eq. (7) is arranged and is not provided, respectively. The truss model representing the load transfer mechanism of horizontal and

15

vertical shear reinforcement has not yet proposed by the ACI 318-05. This means that shear reinforcement satisfying Eq. (7) enables strength of beams to be increased by 25% merely.

Comparisons between test results and predictions obtained from the strut-and-tie model recommended by ACI 318-05 as developed above are shown in Table 3 and Fig. 11: Fig. 11 (a) for simple deep beams given in appendix A and Fig. 11 (b) for continuous deep beams including Rogowsky et al.'s and Ashour's test results. In simple deep beams, the width of strut can be calculated from $w_t'\cos\theta + (l_p)_E \sin\theta$, and the total load is $2F_E \sin\theta$. Although Eq. (7) proposed by ACI 318-05 is recommended for deep beams having concrete strength of less than 40 MPa, the load capacity of H-series beams were also predicted using this equation to evaluate its conservatism in case of high-strength concrete deep beams. The mean and standard deviation of the ratio, $(P_n)_{Exp.}/(P_n)_{ACI}$, between the experimental and predicted load capacities are 1.229 and 0.326, respectively, for simply supported deep beams, and 0.969 and 0.306, respectively, for two-span continuous deep beams as shown in Fig. 11 (b). The ratio of the test result to prediction generally dropped with the increase of a/h ratio. This decrease rate was more remarkable in continuous deep beams than that in simple ones. Especially, the predictions for several continuous deep beams having a/h exceeding 1.0 were unconservative, even though the effectiveness factor used in the beams with either horizontal or vertical shear reinforcement was 0.6 regardless of the amount of shear reinforcement. In addition, for high-strength concrete continuous deep beams having a/h=1.0, the ratio, $(V_n)_{I-Exp.}/(V_n)_{I-ACI}$, between the experimental and predicted shear capacity in the interior shear span were generally below 1.0, as given in Table 3; namely, the strut-and-tie model recommended by ACI 318-05 overestimated the shear capacity of high-strength concrete continuous deep beams having a/h=1.0,.

CONCLUSIONS

Tests were performed to study the influence of the amount and configuration of shear reinforcement on the structural behaviour of continuous deep beams according to the variation of concrete strength and shear span-to-overall depth ratio. The following conclusions are drawn:

1. In beams having shear span-to-overall depth ratio of 0.6, only horizontal shear reinforcement reached its yield strength with sharp increase of stress after the first diagonal crack. Whereas in beams with shear span-to-overall depth ratio of 1.0, only vertical shear reinforcement yielded.

2. For deep beams without shear reinforcement, the normalized ultimate shear strength was 26% lower in continuous beams than that in simple ones. However, when shear reinforcement was provided, the normalized ultimate shear strength in continuous deep beams matched that in simply supported deep beams.

3. The load transfer capacity of all shear reinforcement was much more prominent in continuous deep beams than that in simple ones. Horizontal shear reinforcement was always more effective than vertical shear reinforcement when the shear span-to-overall depth ratio was 0.5. However, vertical shear reinforcement was more effective for shear span-to-overall depth ratios higher than 1.0.

4. In deep beams with shear span-to-overall depth ratios not exceeding 0.6, the critical upper bound on shear strength suggested in ACI 318-05, $0.83\sqrt{f_c'}b_w d$, highly underestimated that measured for beams, as if it was a lower limit.

5. The ratios of measured load capacity to that obtained from the strut-and-tie model recommended by ACI 318-05 dropped with the increase of the shear span-to-overall depth ratio. This decrease rate was more remarkable in continuous deep beams than that in simple ones. The strut-and-tie model recommended by ACI 318-05 overestimated the shear capacity

17

of high-strength concrete continuous deep beams having shear span-to-overall depth ratios more than 1.0.

ACKNOWLEDGMENTS

NOTATION

A_h = area of horizontal shear reinforcement

A_{st} = area of longitudinal bottom reinforcement

A_{st}' = area of longitudinal top reinforcement

A_s = area of shear reinforcement

a = shear span

b_w = width of beam section

c = cover of longitudinal bottom reinforcement

c' = cover of longitudinal top reinforcement

h = overall depth of beam section

E_s = elastic modulus of steel

F_E = load capacity of concrete strut in exterior shear span

F_I = load capacity of concrete strut in interior shear span

f_c' = concrete compressive strength

f_y = yield strength of reinforcement

f_{su} = tensile strength of reinforcement

jd = distance between the center of top and bottom nodes

L = span length

P_{cr} = diagonal crack load

P_n = ultimate load at failure

s_h = spacing of horizontal shear reinforcement

s_v = spacing of vertical shear reinforcement

19

V_{cr} = diagonal crack shear force

V_n = ultimate shear force at failure

w_s = width of concrete strut

α = angle between shear reinforcement and the axis of cocrete strut

β = ratio of exterior reaction to the applied load

ε_y = yield strain of reinforcement

λ = normalized ultimate shear stress

θ = angle between concrete strut and longitudinal axis of beam

ρ_h = horizontal shear reinforcement ratio $\left(\dfrac{A_h}{b_w s_h} \right)$

ρ_{st} = longitudinal bottom reinforcement ratio $\left(\dfrac{A_{st}}{b_w d} \right)$

ρ_{st}' = longitudinal top reinforcement ratio $\left(\dfrac{A_{st}'}{b_w d} \right)$

ρ_v = vertical shear reinforcement ratio $\left(\dfrac{A_v}{b_w s_v} \right)$

v_e = effectiveness factor

REFERENCES

1. Rogowsky, D. M., and MacGregor, J. G., and Ong, S. Y., "Tests of Reinforced Concrete Deep Beams, " ACI Journal, V. 83, No. 4, July-Aug. 1986, pp. 614-623.

2. Ashour, A. F., "Tests of Reinforced Concrete Continuous Deep Beams," ACI Structural Journal, V. 94, No. 1, Jan.-Feb. 1997, pp. 3-12.

3. Subedi, N. K., "Reinforced Concrete Two-Span Continuous Deep Beams," Proc. Instn Civ. Engrs Structs & Bldgs, V. 128, Feb. 1998, pp. 12-25.

4. Tan, K. H., Kong, F. K., Teng, S., and Weng, L. W., "Effect of Web Reinforcement on High-Strength Concrete Deep Beams," ACI Structural Journal, V. 94, No. 5, Sep.-Oct. 1997, pp. 572-582.

5. Smith, K. N., and Vantsiotis, A. S., "Shear Strength of Deep Beams," ACI Journal, V. 79, No. 3, May-June 1982, pp. 201-213.

6. ACI Committee 318: Building Code Requirements for Structural Concrete (ACI 318-05) and Commentary (ACI 318R-05). American Concrete Institute, 2005.

7. Canadian Standards Association (CSA), A23.3-94, Design of Concrete Structures, Canadian Standards Association, Rexdale, Dec., 1994.

8. FIP Recommendations: Practical Design of Structural Concrete. 1999.

9. MacGregor, J. G., Reinforced Concrete : Mechanics and Design, Prentice-Hall International, Inc. 1997.

10. Marti, P., "Basic Tools of Reinforced Concrete Beam Design." ACI Journal, V. 82, No. 1, Jan.-Feb. 1985, pp. 46-56.

11. Schlaich, J. and Schafer, K., "Toward a Consistent Design of Structural Concrete," PCI Journal, V. 32, No. 3, May-June 1987, pp. 74-150.

12. Tjhin, T. N., and Kuchma, D. A., 'Example 1b: Alternative Design for the Non-Slender Beam (Deep Beam)' in Reineck, K. H. (ed.), Examples for the Design of Structural Concrete with Strut-and-Tie Models, ACI International SP-208, 2002, pp. 81-90.

13. Yang, K. H., Evaluation on the Shear Strength of High-Strength Concrete Deep Beams, Ph. D. Thesis, Chungang University, Korea, Feb. 2002, 120 pp.

14. Červenka, V., and Červenka, J., ATENA Computer Program for Non-Linear FEM Analysis of Reinforced Concrete Structures, Cervenka Consultant, 2003.

15. ACI Committee 318: Building Code Requirements for Structural Concrete (ACI 318-99) and Commentary (ACI 318R-99). American Concrete Institute, 1999.

APPENDIX A

Table A.1 – Details and test results of simple deep beams (Yang[13])

Simple	f_c' MPa	a/h	a/jd	ρ_h	ρ_v	V_{cr} kN	P_n, kN		$\dfrac{(P_n)_{EXP.}}{(P_n)_{ACI}}$
							Exp.	ACI 318-05	
No.1				0	0	254.0	958.0	684.1	1.400
No.2				0	0.006	259.0	992.0	684.1	1.450
No.3		0.5	0.59	0	0.012	260.0	1111.3	684.1	1.624
No.4				0.006	0	249.9	1042.7	684.1	1.524
No.5				0.006	0.006	262.6	1323.0	855.2	1.547
No.6				0.012	0	270.5	1391.6	684.1	2.034
No.7				0	0.006	188.0	876.1	624.7	1.402
No.8		0.7	0.82	0.006	0	215.6	993.7	624.7	1.591
No.9	31.4			0.006	0.006	205.8	1044.7	780.9	1.338
No.10				0	0	173.5	750.7	520.0	1.444
No.11				0	0.006	172.5	762.4	520.0	1.466
No.12				0	0.012	195.0	1107.4	520.0	2.130
No.13		1.0	1.18	0.006	0	178.4	601.7	520.0	1.157
No.14				0.006	0.006	181.0	905.5	650.0	1.393
No.15				0.012	0	185.0	707.6	520.0	1.361
No.16		1.5	1.76	0	0	107.8	409.6	378.8	1.081
No.17				0.006	0.006	142.1	721.3	473.5	1.523
No.18		0.5	0.59	0	0	290.0	1540.6	1154.5	1.334
No.19	52.9			0.006	0.006	318.5	1775.8	1443.1	1.230
No.20		1.0	1.18	0	0	225.4	952.6	877.4	1.086
No.21				0.006	0.006	245.0	1129.0	1096.8	1.029
No.22				0	0	347.9	1646.4	1710.4	0.963
No.23				0	0.006	357.7	1789.5	1710.4	1.046
No.24		0.5	0.59	0	0.012	347.9	1934.5	1710.4	1.131
No.25				0.006	0	392.0	1962.0	1710.4	1.147
No.26				0.006	0.006	345.0	2061.9	2138.0	0.964
No.27				0.012	0	401.8	2269.7	1710.4	1.327
No.28				0	0.006	289.1	1622.9	1561.8	1.039
No.29		0.7	0.82	0.006	0	303.8	1395.5	1561.8	0.894
No.30	78.4			0.006	0.006	308.7	1701.3	1952.2	0.871
No.31				0	0	254.8	1146.6	1299.9	0.882
No.32				0	0.006	240.1	1356.3	1299.9	1.043
No.33				0	0.012	294.0	1558.2	1299.9	1.199
No.34		1.0	1.18	0.006	0	249.9	1213.2	1299.9	0.933
No.35				0.006	0.006	281.3	1295.6	1624.9	0.797
No.36				0.012	0	291.1	1215.2	1299.9	0.935
No.37		1.5	1.76	0	0	173.5	656.6	947.0	0.693
No.38				0.006	0.006	181.3	836.9	1183.7	0.707
Mean									1.229
Standard deviation									0.326

psi = MPa/145; kips = kN/4.4481.

TABLES AND FIGURES

List of Tables:

List of Figures:

Table 1–Details of Test Specimens

Specimen	$f_c^{'}$, MPa	a/h	a/jd	L mm	Details of Shear reinforcement			
					Horizontal		Vertical	
					s_h, mm	ρ_h	s_v, mm	ρ_v
L5NN	32.4	0.5	0.58	600	-	-	-	-
L5NS					-	-	120	0.003
L5NT					-	-	60	0.006
L5SN					120	0.003	-	-
L5SS					120	0.003	120	0.003
L5TN					60	0.006	-	-
L10NN	32.1	1.0	1.17	1200	-	-	-	-
L10NS					-	-	120	0.003
L10NT					-	-	60	0.006
L10SN					120	0.003	-	-
L10SS					120	0.003	120	0.003
L10TN					60	0.006	-	-
H6NN	65.1	0.6	0.7	720	-	-	-	-
H6NS					-	-	120	0.003
H6NT					-	-	60	0.006
H6SN					120	0.003	-	-
H6SS					120	0.003	120	0.003
H6TN					60	0.006	-	-
H10NN	68.2	1.0	1.17	1200	-	-	-	-
H10NS					-	-	120	0.003
H10NT					-	-	60	0.006
H10SN					120	0.003	-	-
H10SS					120	0.003	120	0.003
H10TN					60	0.006	-	-

psi = MPa/145; in. = mm/25.4.

Table 2–Mechanical properties of reinforcement

Diameter, mm	f_y, MPa	ε_y	f_{su}, MPa	E_s, GPa
6[*]	483	0.0044	549	199
19	562	0.00284	741	198

* The yield stress of 6 mm diameter reinforcement was obtained by 0.2 % offset method.

psi = MPa/145.

TABLE 3-Details of test results and predictions obtained from ACI 318-05

Specimen	Load (P_{cr}) and shear force (V_{cr}) at the first diagonal crack, kN								Failure load (P_n) and Ultimate shear force (($V_n)_I$) at the interior shear spans, kN			ACI 318-05		$\dfrac{(P_n)_{Exp.}}{(P_n)_{ACI}}$	$\dfrac{(V_n)_{I-Exp.}}{(V_n)_{I-ACI}}$
	W-span				E-span				P_n	$(V_n)_I$		P_n	$(V_n)_I$		
	Interior		Exterior		Interior		Exterior			W-span	E-span	kN	kN		
	$(P_{cr})_I$	$(V_{cr})_I$	$(P_{cr})_E$	$(V_{cr})_E$	$(P_{cr})_I$	$(V_{cr})_I$	$(P_{cr})_E$	$(V_{cr})_E$							
L5NN	852	255	902	180	816	244	937	187	1635	473	456*	1298	342	1.260	1.334
L5NS	849	247	1028	210	857	262	1330	281	1710	486	475*	1298	342	1.317	1.389
L5NT	1017	278	1380	284	850	230	1260	262	1789	512*	494	1298	342	1.378	1.498
L5SN	864	255	1268	252	867	257	927	179	1887	537*	546	1298	342	1.454	1.571
L5SS	814	247	990	192	980	293	1020	202	2117	607*	583	1623	427	1.305	1.420
L5TN	912	266	1130	230	910	278	966	185	2317	655	640*	1298	342	1.785	1.872
L10NN	537	173	-	-	537	171	-	-	880	264*	262	1000	265	0.880	0.997
L10NS	477	156	-	-	596	195	-	-	1153	349	348*	1000	265	1.153	1.314
L10NT	635	206	1023	230	647	208	-	-	1541	446*	439	1000	265	1.541	1.684
L10SN	498	153	-	-	490	151	782	146	884	266	265*	1000	265	0.884	1.000
L10SS	521	166	-	-	452	148	713	129	1177	357	352*	1250	331	0.942	1.063
L10TN	538	175	--	--	621	193	775	143	935	287	288*	1000	265	0.935	1.087

Specimen	Load (P_{cr}) and shear force (V_{cr}) at the first diagonal crack, kN								Failure load (P_n) and Ultimate shearing force ($(V_n)_I$) at the interior shear spans, kN			ACI 318-05		$\dfrac{(P_n)_{Exp.}}{(P_n)_{ACI}}$	$\dfrac{(V_n)_{I-Exp.}}{(V_n)_{I-ACI}}$
	W-span				E-span					$(V_n)_I$					
	Interior		Exterior		Interior		Exterior		P_n	W-span	E-span	P_n	$(V_n)_I$		
	$(P_{cr})_I$	$(V_{cr})_I$	$(P_{cr})_E$	$(V_{cr})_E$	$(P_{cr})_I$	$(V_{cr})_I$	$(P_{cr})_E$	$(V_{cr})_E$				kN	kN		
H6NN	1046	305	1562	321	1236	303	1960	407	2248	633*	634	2520	668	0.892	0.950
H6NS	1261	379	1646	316	978	300	2280	457	2289	684	683*	2520	668	0.908	1.023
H6NT	1116	324	2550	550	915	264	2480	531	2625	757	757*	2520	668	1.042	1.134
H6SN	1322	393	2420	517	1022	297	2420	513	2427	703*	708	2520	668	0.963	1.053
H6SS	1207	367	2630	548	825	256	2630	542	2763	792	799*	3150	834	0.877	0.958
H6TN	1442	439	-	-	980	297	2648	540	2966	854	852*	2520	668	1.177	1.276
H10NN	690	228	868	149	690	228	840	143	1276	373	372*	2124	563	0.601	0.661
H10NS	759	237	-	-	751	234	-	-	1443	413*	414	2124	563	0.679	0.734
H10NT	788	251	-	-	717	224	-	-	2116	638	637*	2124	563	0.996	1.132
H10SN	757	255	-	-	757	252	-	-	1309	387*	378	2124	563	0.616	0.688
H10SS	718	232	-	-	768	244	-	-	1575	492*	484	2655	703	0.593	0.699
H10TN	754	234	-	-	704	220	-	-	1287	393	388*	2124	563	0.606	0.689
Mean														1.033	1.134
Standard deviation														0.320	0.330

* Failure occurred in this shear span. kips = kN/4.4481.

(a) Beam without shear reinforcement

(b) Beam with horizontal reinforcement only

(c) Beam with vertical reinforcement only

(d) Beam with orthogonal reinforcement
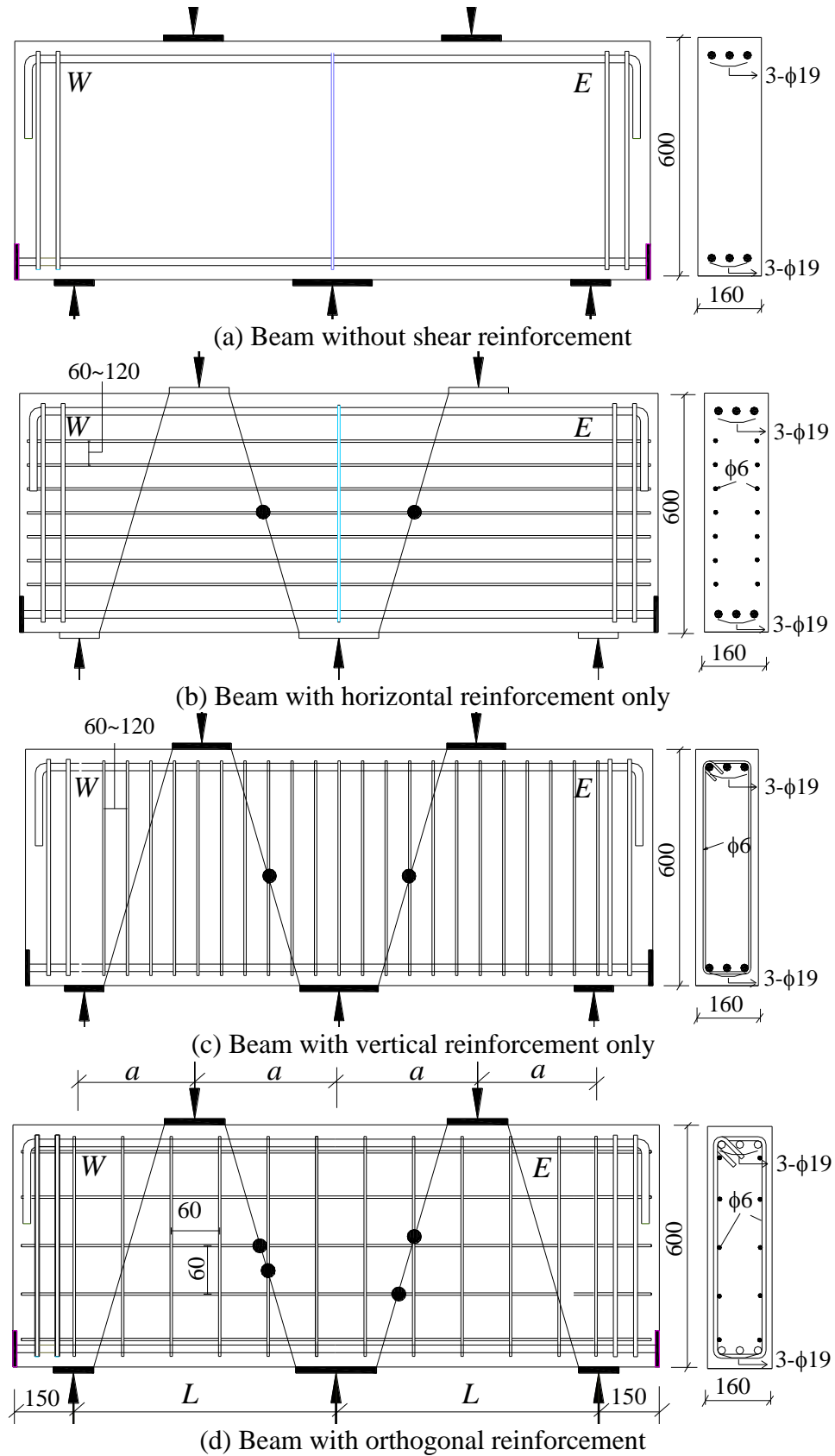
Fig. 1-Geometrical dimensions and reinforcement of test specimens.

(All dimensions are in mm (=in. $\times$ 25.4), and $\bullet$ indicate the locations of strain gages)
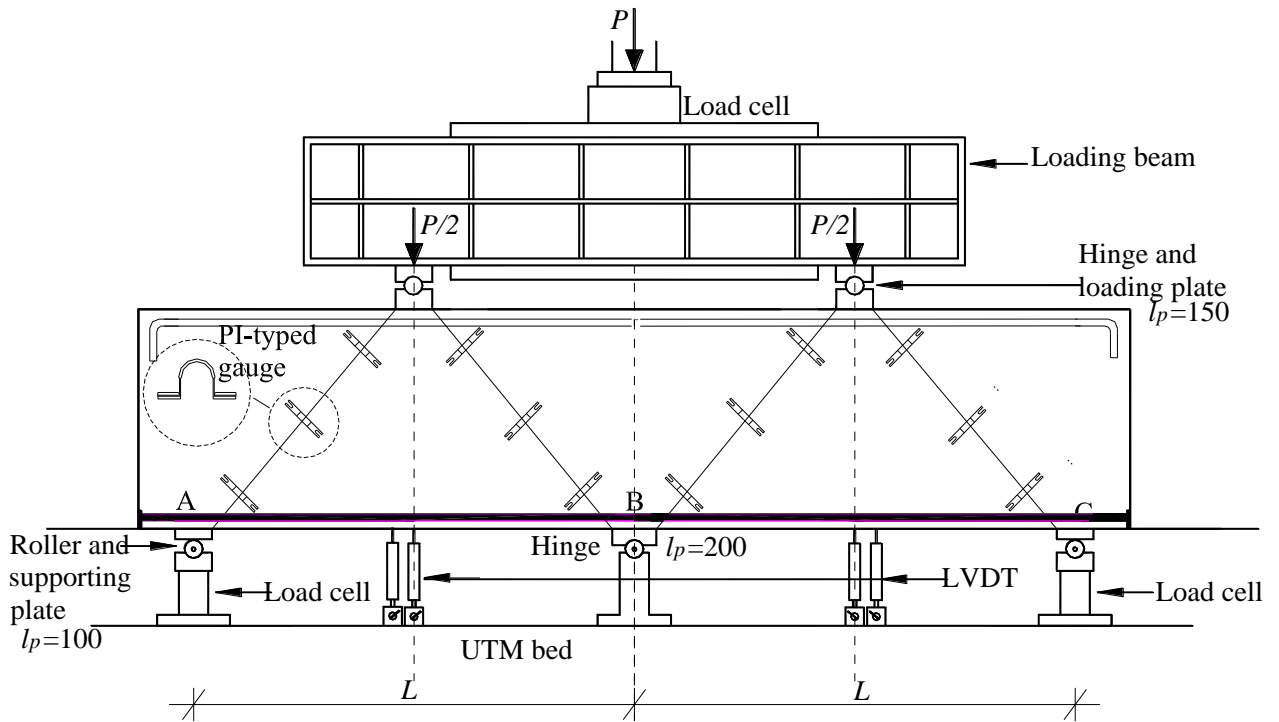
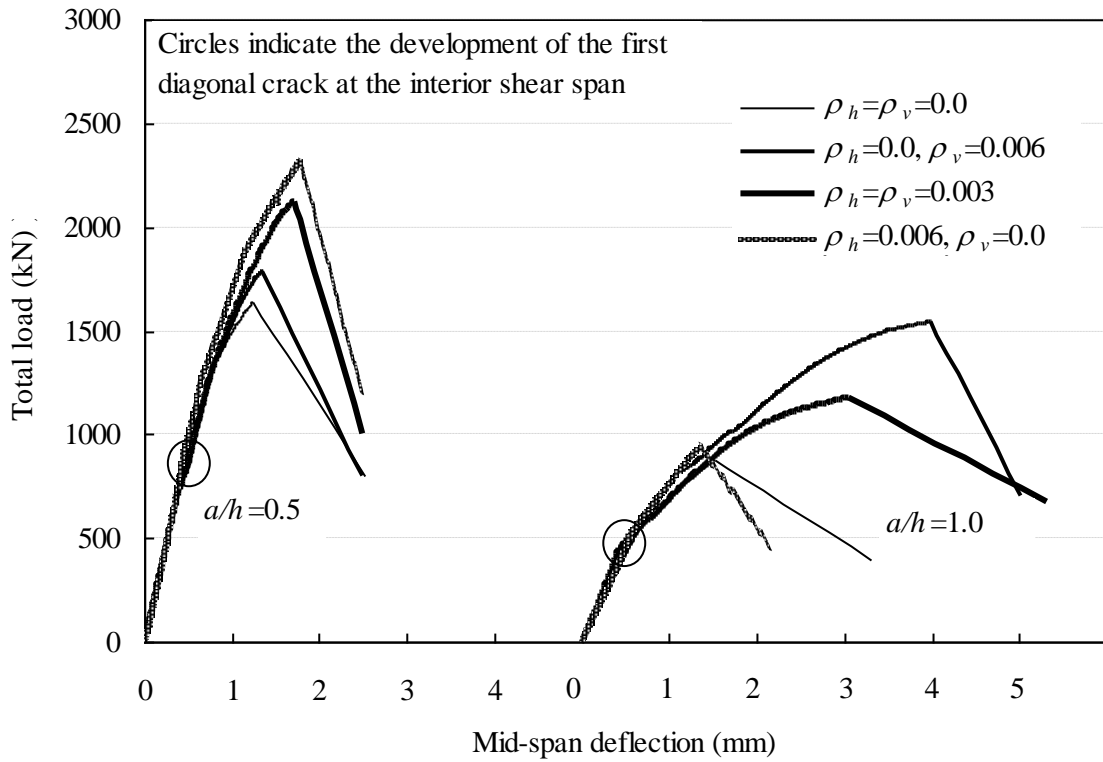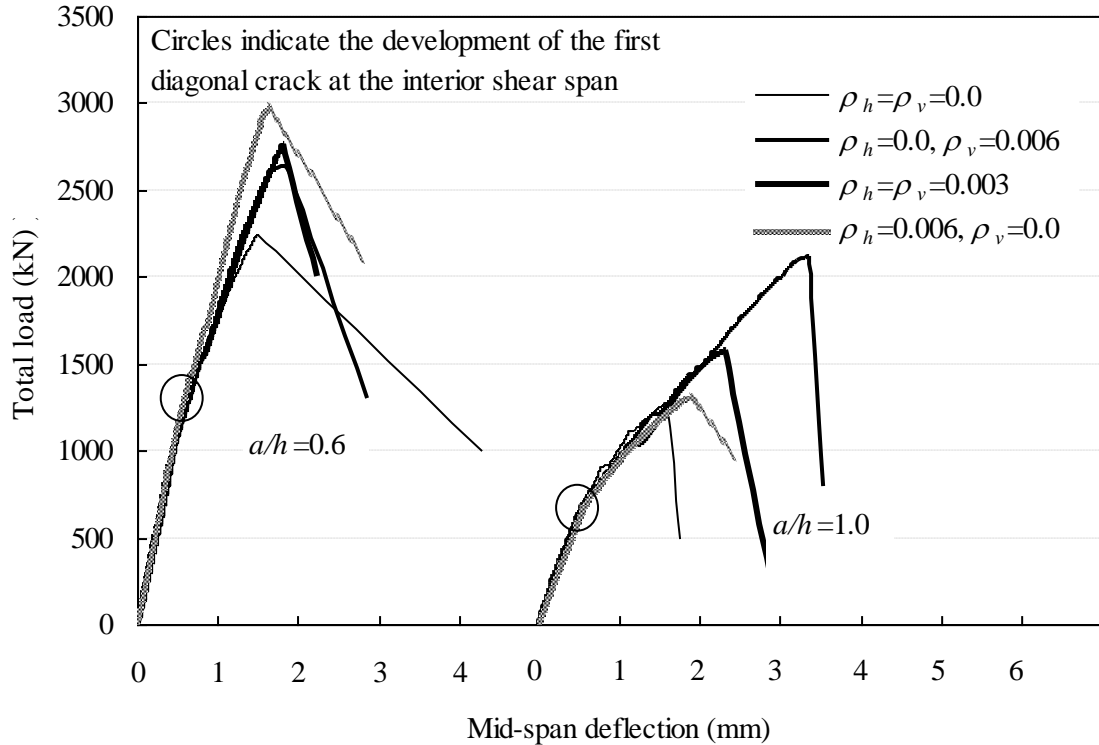**Fig. 2-Test set-up (all dimensions are in mm (= in. $\times$ 25.4).**
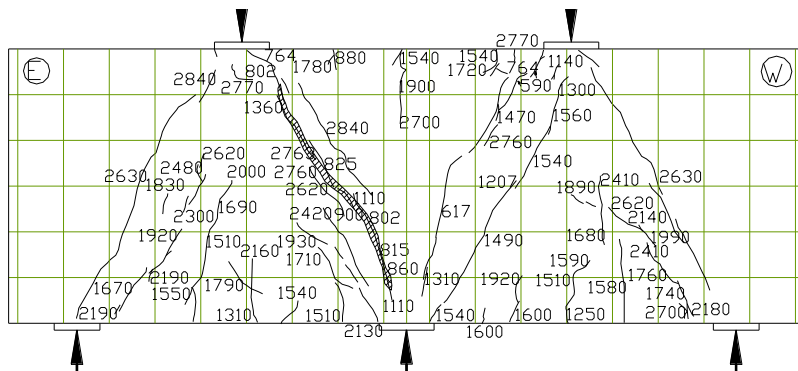
(a) H6SS
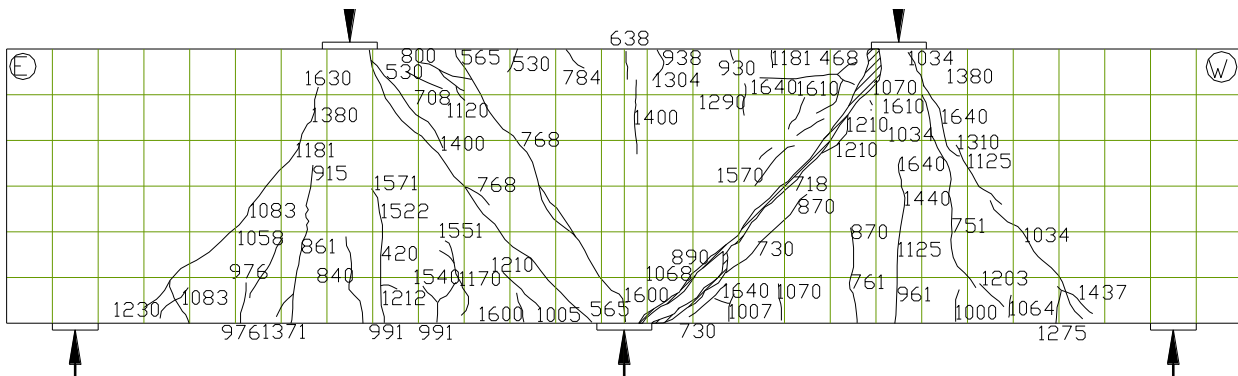
(b) H10SS

Fig. 3–Crack patterns and failure of concrete strut.

(Numbers indicate the total load in kN (= kips × 4.4481) at which crack occurred.)

Circles indicate the development of the first
diagonal crack at the interior shear span

$\rho_h=\rho_v=0.0$
$\rho_h=0.0, \rho_v=0.006$
$\rho_h=\rho_v=0.003$
$\rho_h=0.006, \rho_v=0.0$

a/h =0.5

a/h =1.0

(a) L-series

Circles indicate the development of the first
diagonal crack at the interior shear span

$\rho_h=\rho_v=0.0$
$\rho_h=0.0, \rho_v=0.006$
$\rho_h=\rho_v=0.003$
$\rho_h=0.006, \rho_v=0.0$

a/h =0.6

a/h =1.0

(b) H-series

Fig. 4–Total load versus mid-span deflection. (kips = kN/4.4481)
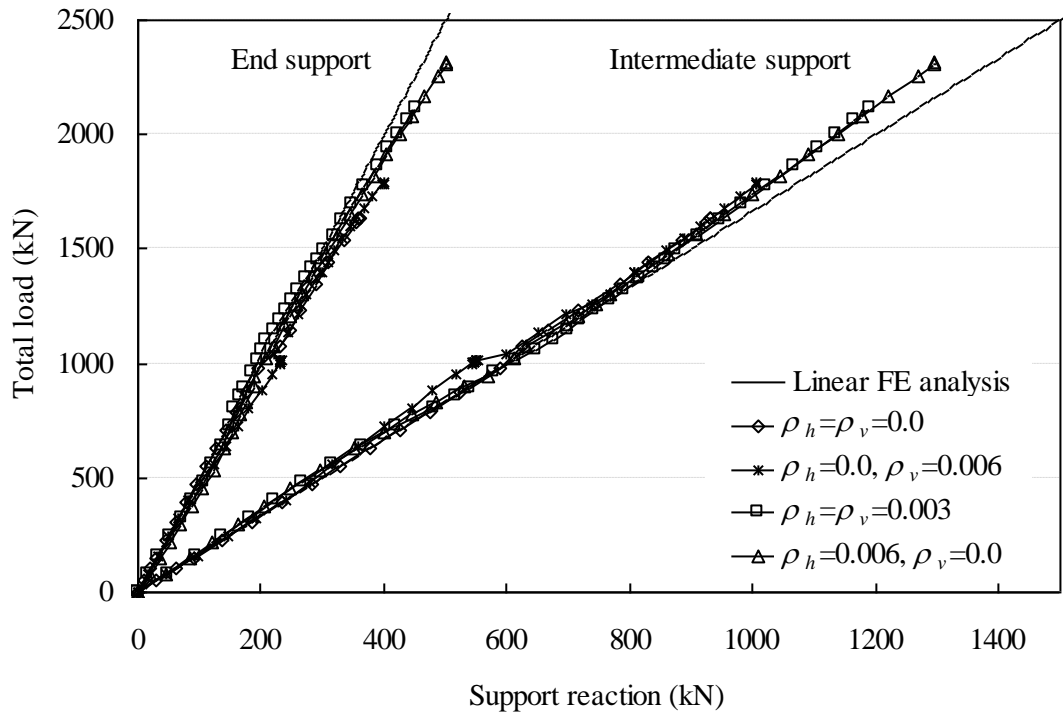
(a) *a/h*=0.5
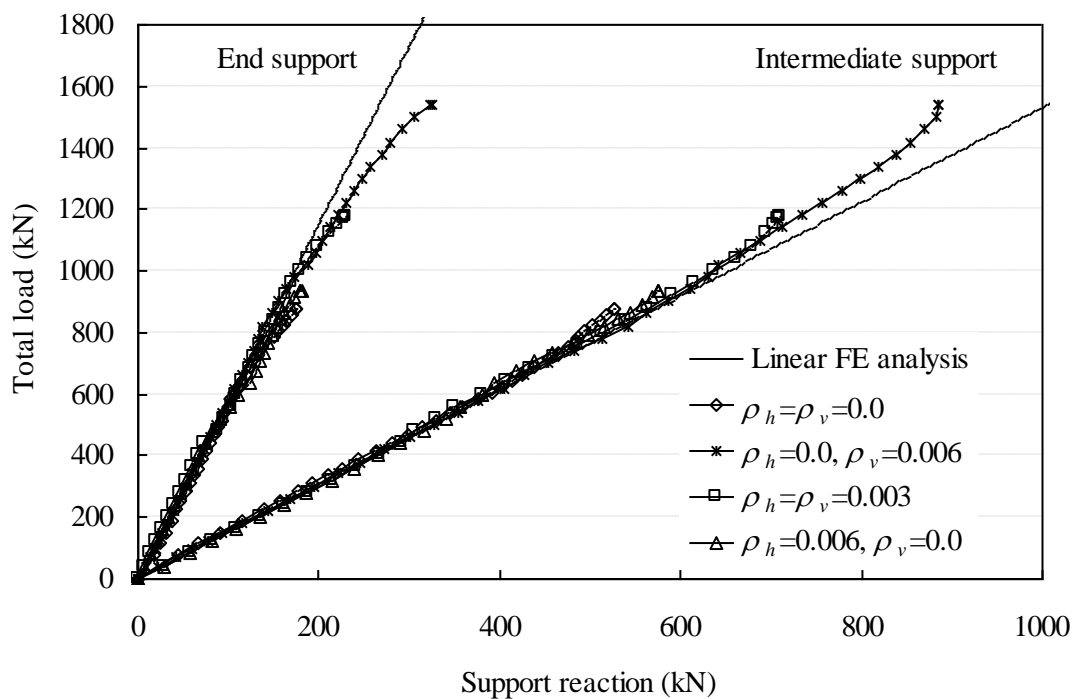
(b) *a/h*=1.0

Fig. 5–Total applied load versus support reactions for beams tested in L-series.

(kips = kN/4.4481)
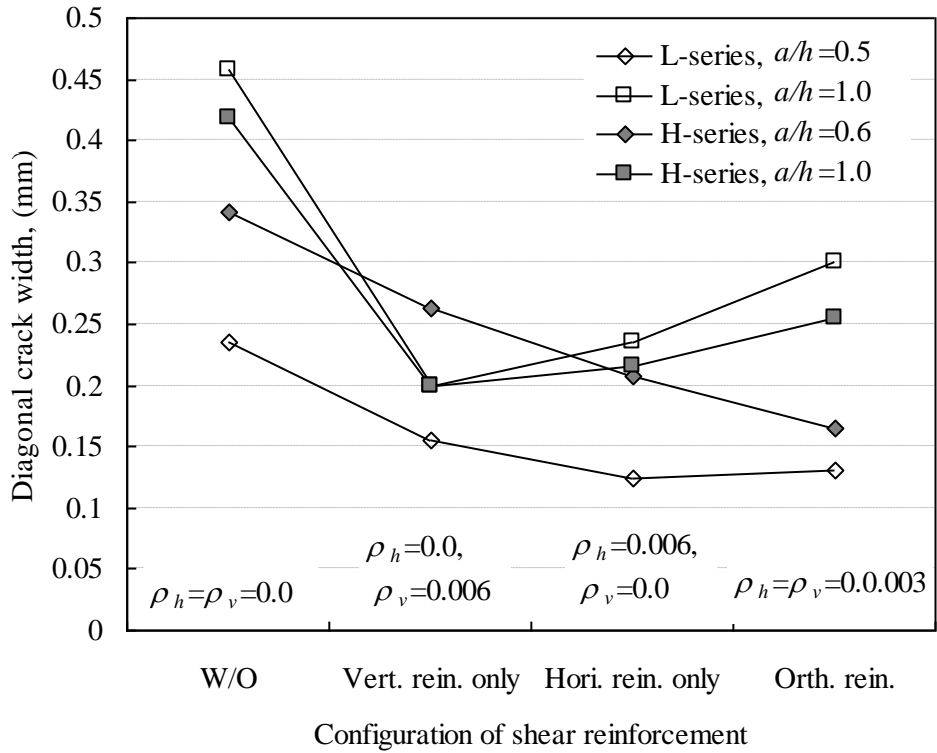
(a) At the first diagonal crack load
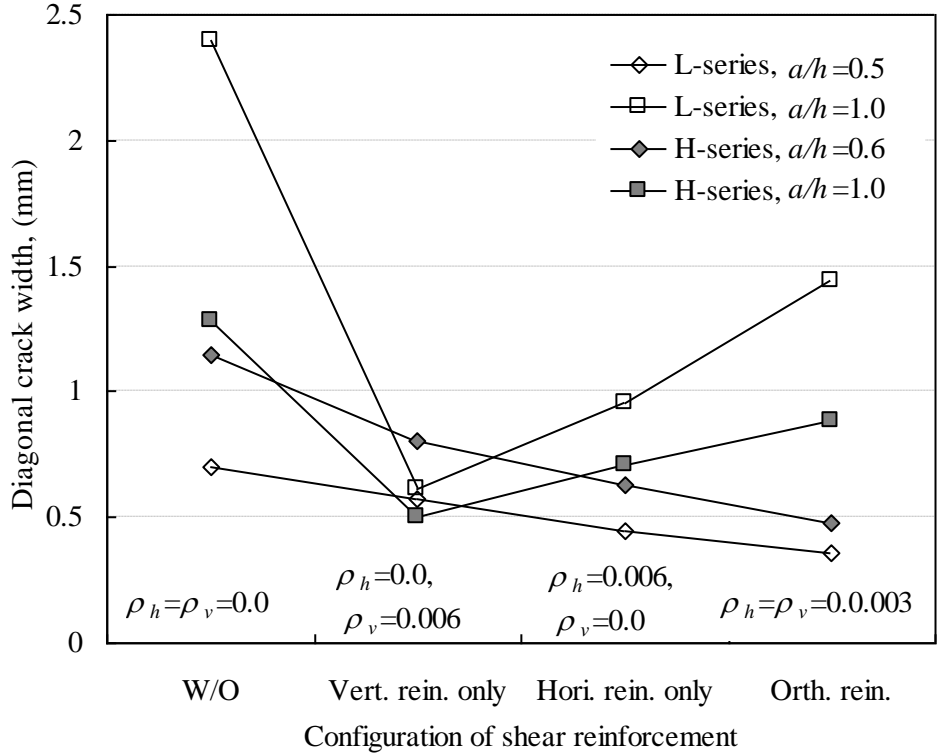
(b) At the same load as the failure load of beams without shear reinforcement

Fig. 6–Configuration of shear reinforcement versus diagonal crack width. (in. = mm/25.4)
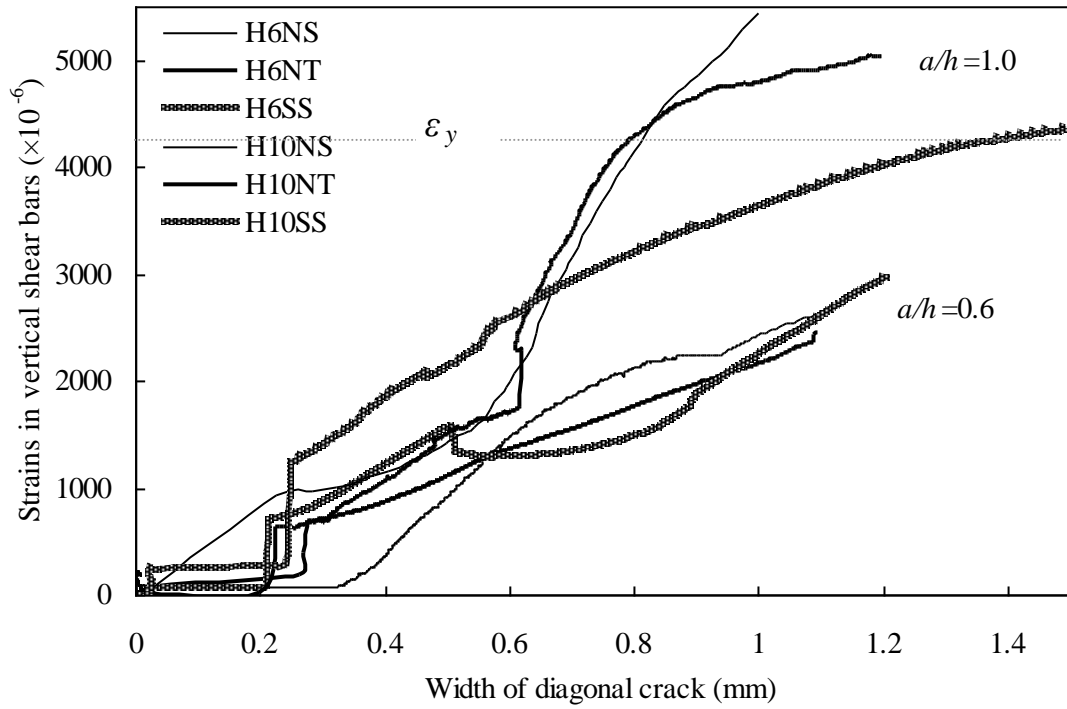
(a) For beams with vertical shear reinforcement only or with orthogonal shear reinforcement
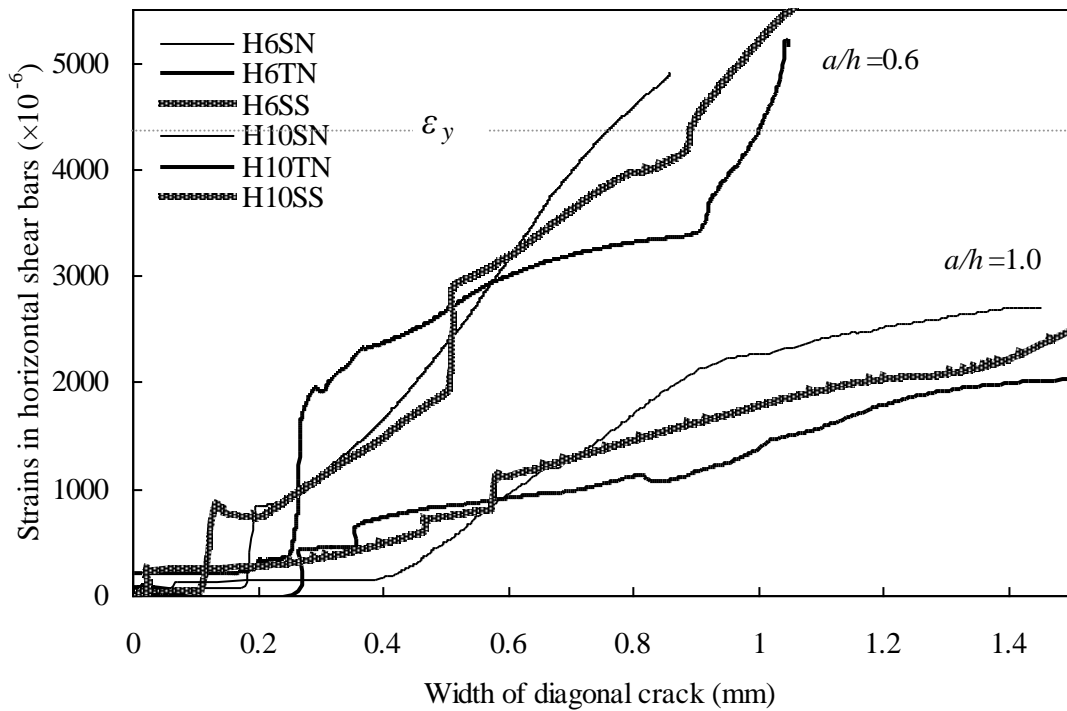
(b) For beams with horizontal shear reinforcement only or with orthogonal shear reinforcement

Fig. 7–Strains in shear reinforcement versus diagonal crack width for beams in H-series.

(in. = mm/25.4)

35
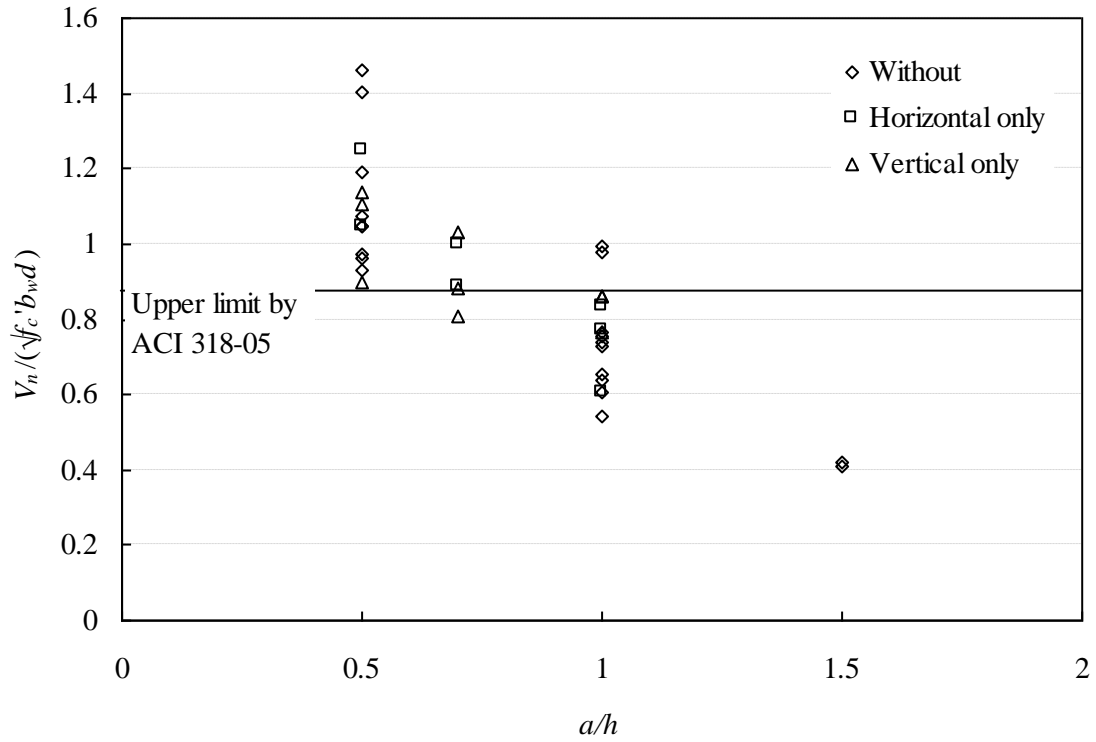
(a) Simple deep beams
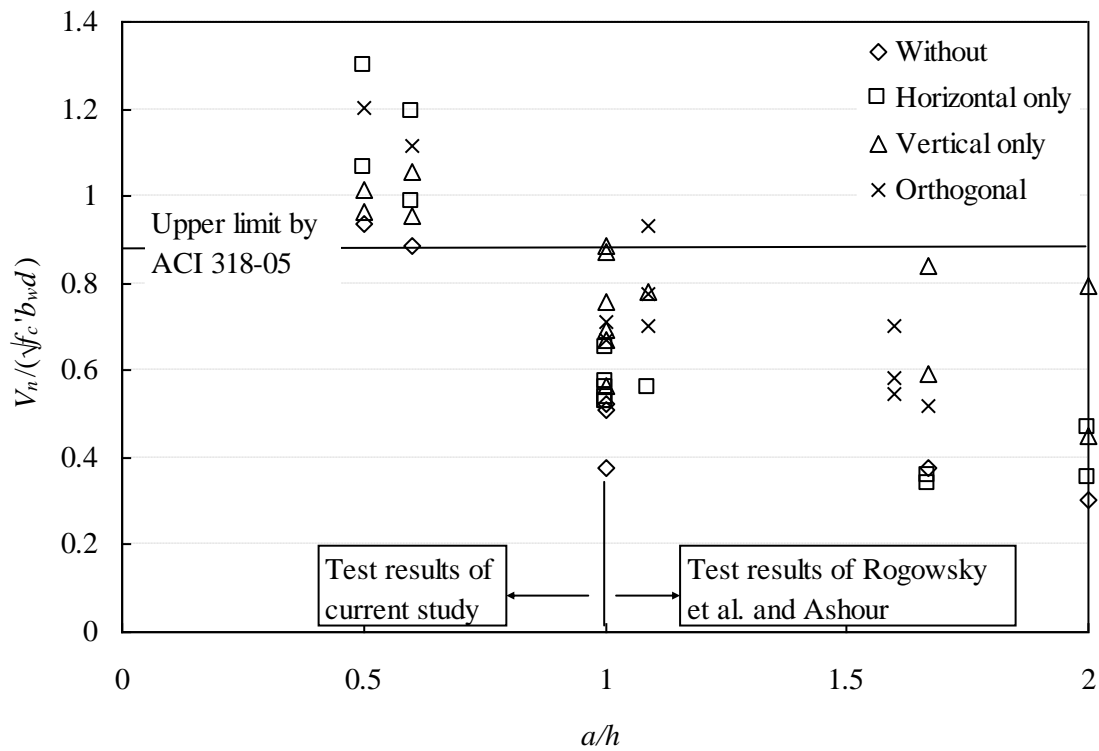
(b) Two-span continuous deep beams

Fig. 8-Normalized ultimate shear strength versus shear span-to-overall depth ratio.
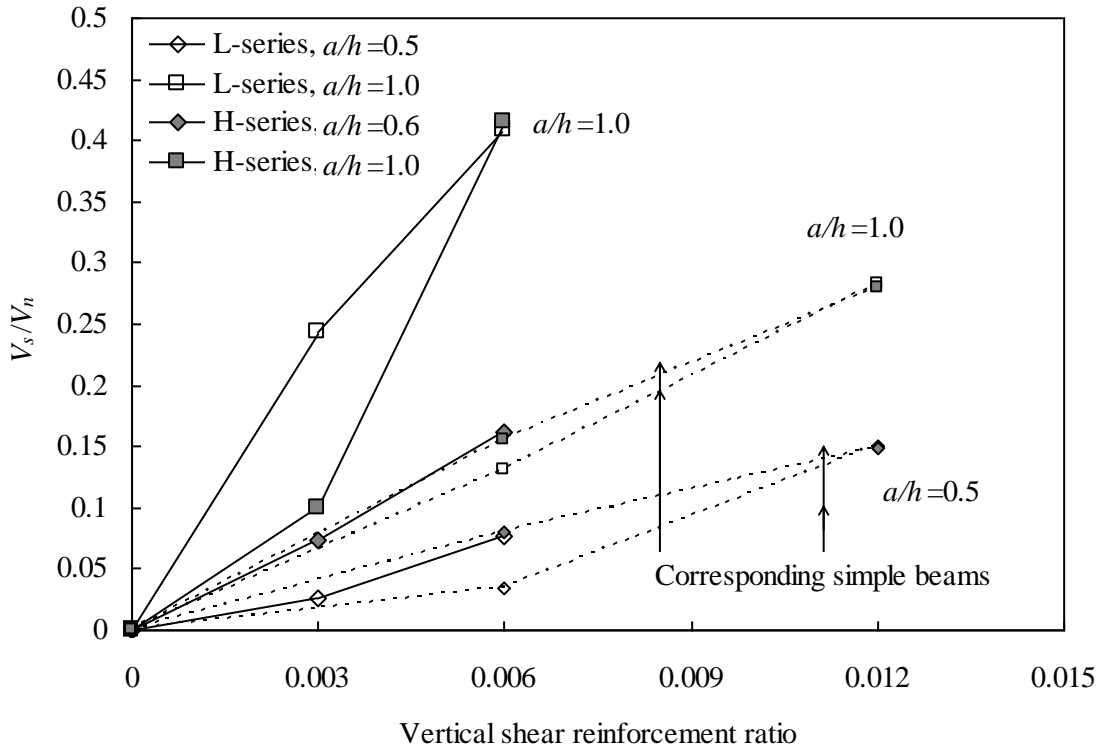
(a) Vertical shear reinforcement only
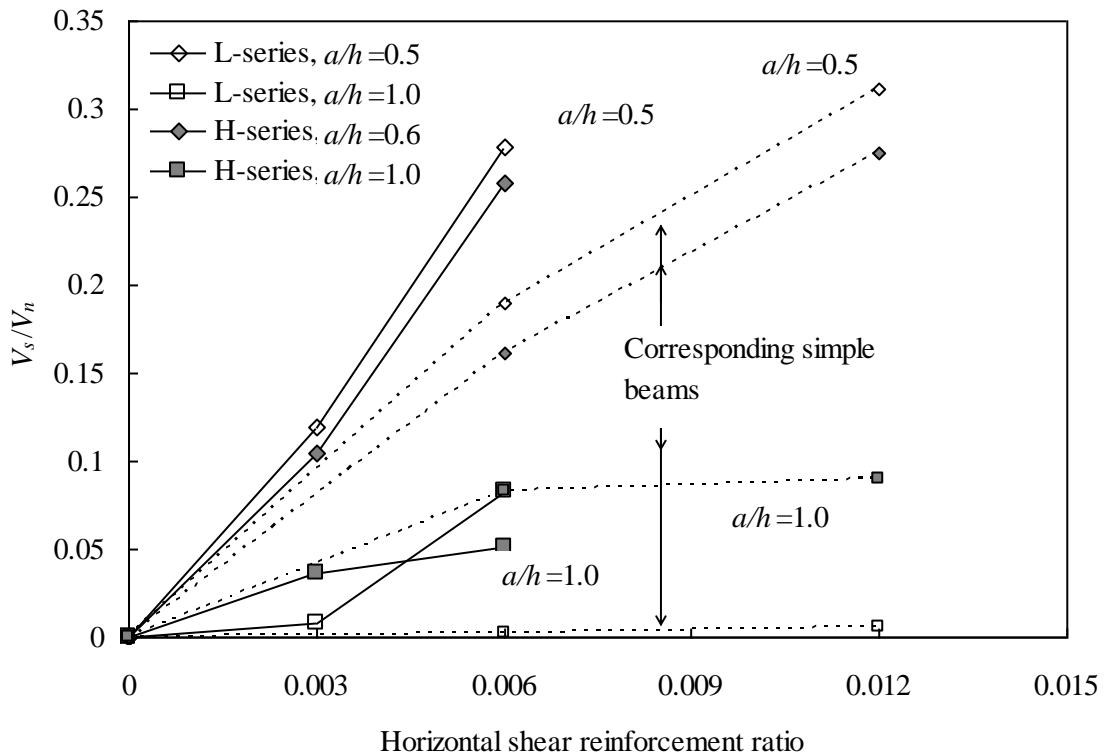
(b) Horizontal shear reinforcement only
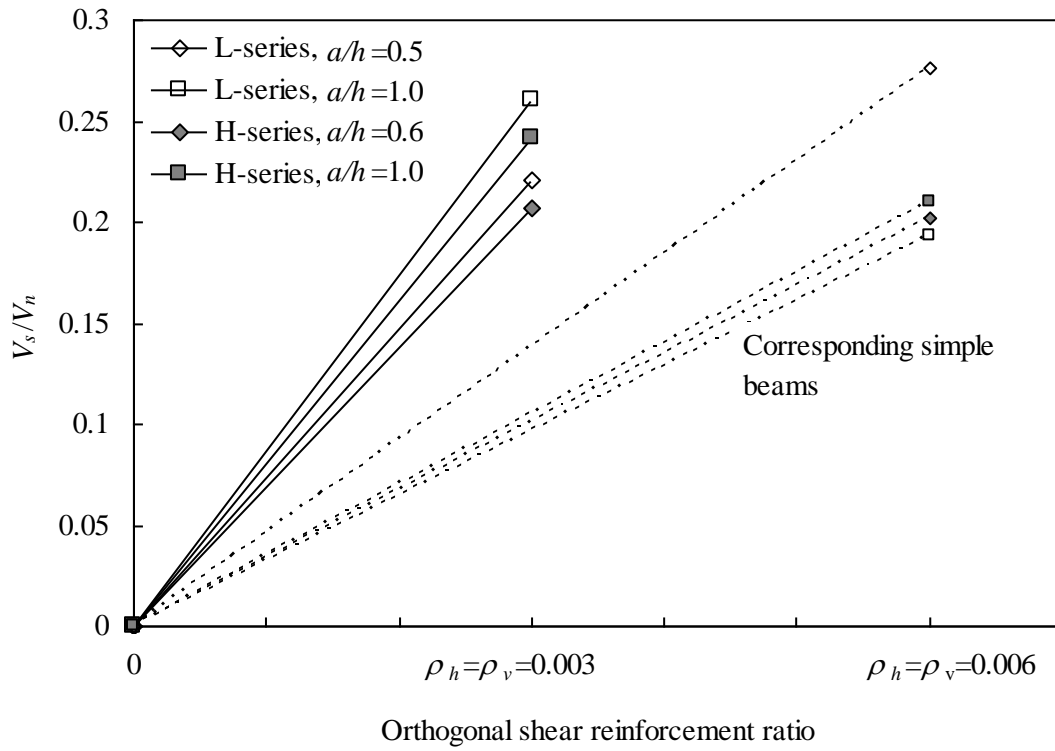
(c) Orthogonal shear reinforcement

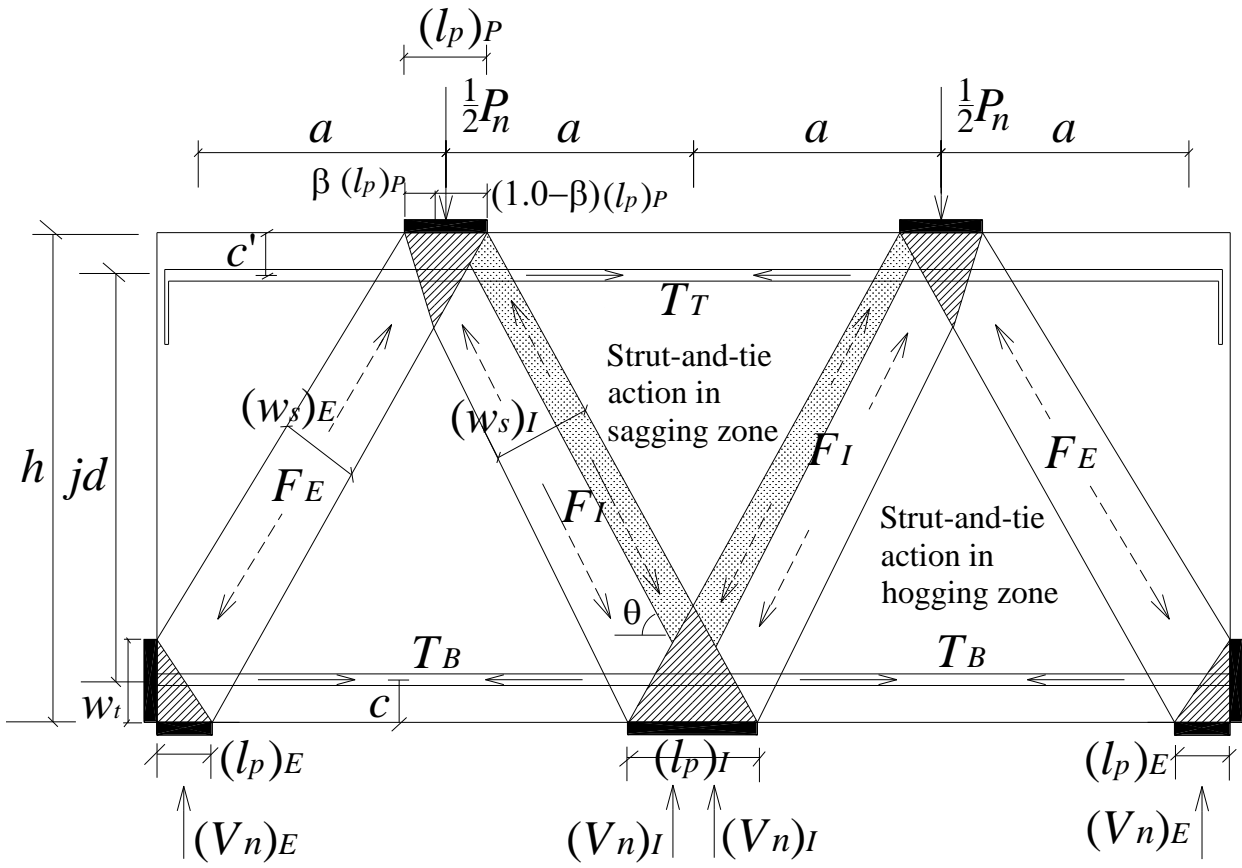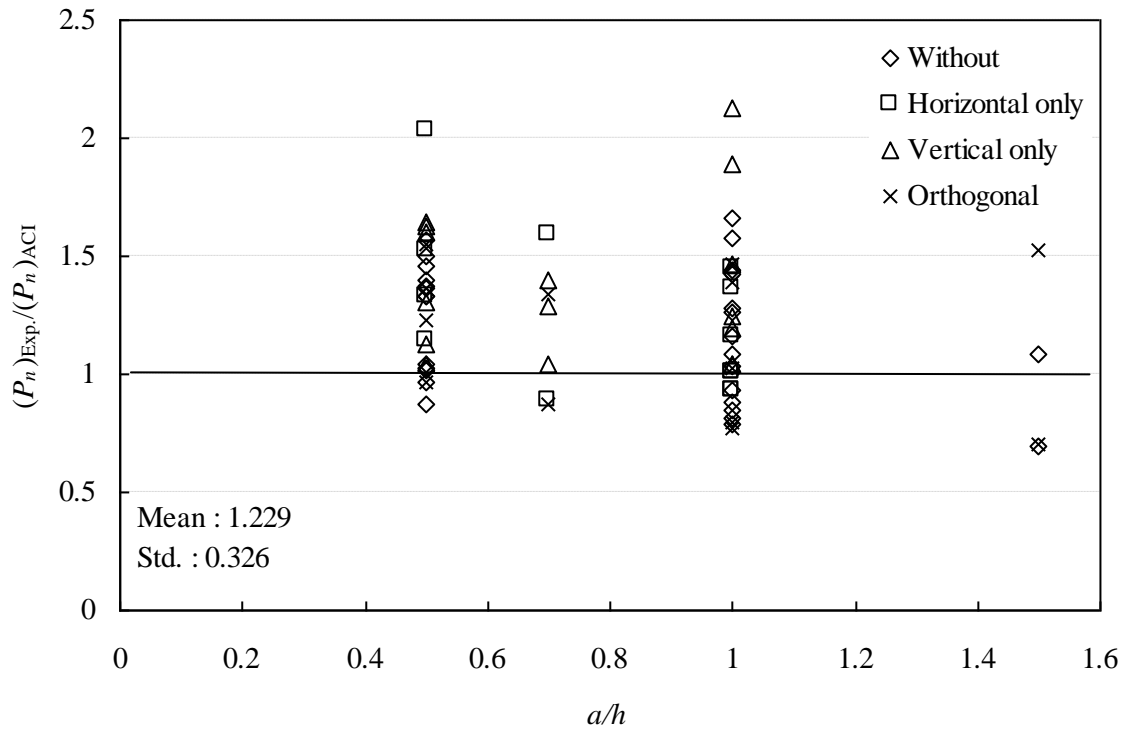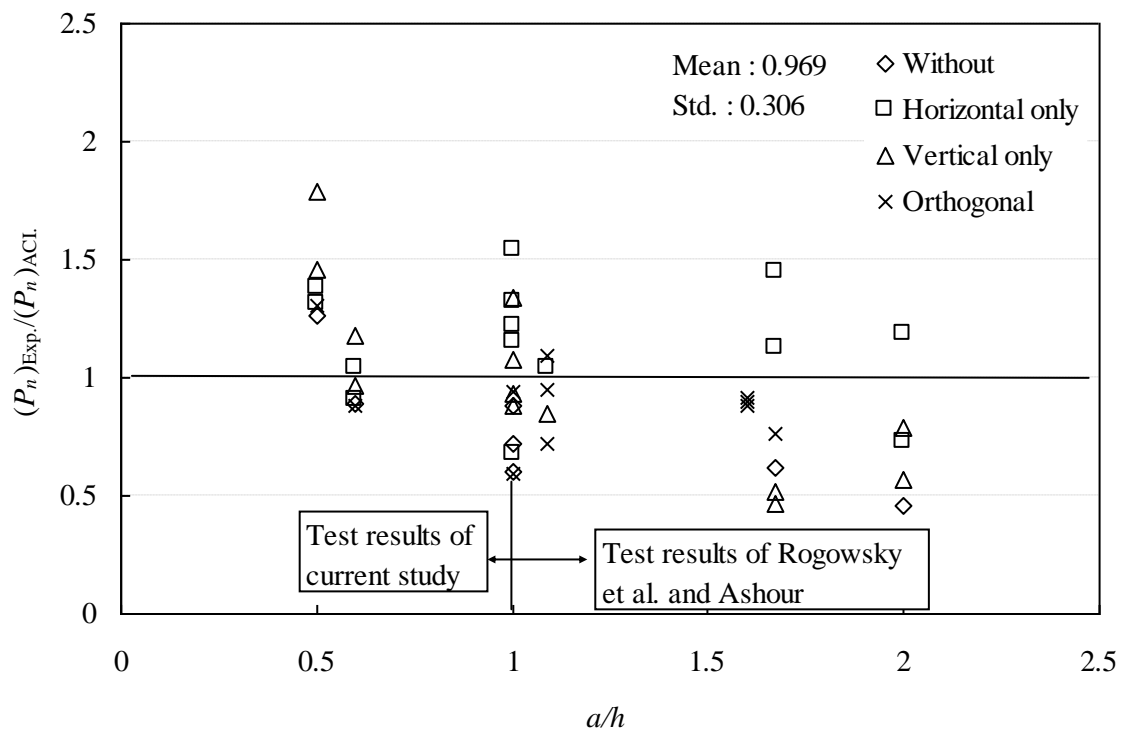**Fig. 9–Shear reinforcement ratios versus V_s/V_n**

Fig. 10- Strut-and-tie model of continuous deep beams according to ACI 318-05.

(a) Simple deep beams

(b) Two-span continuous deep beams

Fig. 11–Comparison of test results and predictions by ACI 318-05.